Published by :
http://www.ijert.org

International Journal of Engineering Research & Technology (IJERT)
ISSN: 2278-0181
Vol. 8 Issue 04, April-2019

Analysis and Experimentation of Grid Integrated PV-Battery System for Residential and Electrical Vehicle Applications

[1]L. Rajamohan, [2]K. Uma Maheswari
Assistant Professor
Department of Electrical Engineering
Chendhuran College of Engineering & Technology
Pudukkottai 622 003

[3]S. Elakkia, [4]D. Priyanka
UG Scholar,
Department of Electrical Engineering
Chendhuran College of Engineering & Technology
Pudukkottai 622 003

***Abstract*- A new control approach of integrating a solar PV (Photovoltaic) with battery storage is presented to a single phase grid for residential and electric vehicle application. Our aim of the proposed work is to increase the security of the system for that we are providing continuous power to the grid thereby enhancing the feasible of the charging and discharging power of storage support battery energy level and load level. In our system, once the alleviation of failure has been achieved it will be automatically rectified in the proposed system. The multifunctional voltage source converter acts as an active power filter and performs the harmonics mitigation along with reactive power compensation. The overall control of the system is adaptable under various practically occurring situations such as disconnection of PV array, battery, and grid from the system. The validity of the proposed system is performed through a laboratory prototype developed for a power rating of 2.2kWconnected to the utility grid. The performance of the system is found satisfactory under various disturbance and the recorded results have been demonstrated.**

Keywords: Solar PV, harmonics mitigation, electric vehicle, grid, energy level, load level

I. INTRODUCTION

A micro-grid is a localized group of electricity sources and loads that normally operate connected to and synchronous with the traditional wide area synchronous grid (micro-grid), but can also disconnect to "island mode" and function autonomously as physical or economic conditions dictate. Always renewable energy sources can supply emergency power and renewable electricity in a micro-grid whereas it is the combination of various sources of distributed generation, changing between the island and connected modes. Control and protection are challenges to micro-grids. A very important feature is also to provide multiple end-user needs as heating, cooling, and electricity at the same time since this allows energy carrier substitution and increased energy efficiency due to domestic hot water, waste heat utilization for heating, and cooling purposes. It can enable to operate in both connected or island-mode from the grid. A micro-grid can connect and disconnect from the grid The EU research project describes a micro-grid as comprising Low-Voltage (LV) distribution systems with distributed energy resources (DERs) (micro-turbines, fuel cells, photovoltaic (PV), etc.), storage devices (batteries, flywheels) energy storage system and flexible loads. From the main grid, it can operate either connected or disconnected for such systems. By using this system it provides an advantage to the overall system performance if managed and well organized.

II. LITERATURE SURVEY

Moacyr Aureliano et.al (2013) The main experimental results are presented for conventional MPPT algorithms and improved MPPT algorithms named IC based on proportional–integral (PI) and perturb and observe based on PI. Moreover, the dynamic response and the TF are also evaluated using a user-friendly interface, which is capable of online program power profiles and computes the TF.

Leopoldo Gil-Antonio at.al (2016) Despite their numerous advantages, PV systems have two major drawbacks: low energy conversion efficiency and loss of energy due to variations in meteorological conditions; for this reason, Maximum Power Point Tracking (MPPT) control techniques play a key role in exploiting the maximum energy caught by PV modules.

Yousef Mahmoud at.al (2016) This paper develops a fast modeling approach for partially shaded PV systems. By utilizing three developed rules that govern the formation of power peaks in partially shaded PV systems, the proposed approach can quickly find the power peaks of these systems without simulating the entire power curve. The effectiveness of the proposed approach in finding the power peaks of PV systems quickly and accurately.

Chinmay Jain et.al (2017) To implement adjustable DC link voltage structure, the reference DC link voltage is adjusted with variation in CPI voltage in real time. A PI (Proportional-Integral) controller is used to regulate DC link voltage to set reference value. A wide range of experimental results are shown to demonstrate the features of proposed system. The THD (Total Harmonics Distortion) of grid current has been found well under IEEE-519 standard even under nonlinear loads at CPI.

Rahul Kumar Agarwal et.al (2016) In order to increase the efficiency and maximum power to be extracted from the SPV array at varying environmental conditions, a single stage system is used along with P&O (Perturb and Observe) method of MPPT (Maximum Power Point Tracking) integrated with the LMF based control technique.

International Journal of Engineering Research & Technology (IJERT)
ISSN: 2278-0181
Vol. 8 Issue 04, April-2019

Liping Pan, Juping Gu et.al(2016) This paper introduces an integrated control strategy of smoothing power fluctuations and peak shaving based on HESS (hybrid storage energy system) with super-capacitor and battery. The generated power fluctuations of the wind/photovoltaic (PV)/HESS will be controlled under constraints by low-pass filter. Meanwhile the grid peak load will be shifted by integration power forecasting with storage plan management of future 24 hours. The integrated control strategy can realize the power smooth and load shifting effectively.

III. PROPOSED SYSTEM

The Proposed system combination of both existing methods has been adopted to develop a novel reactive power controller which can eliminate these shortcomings. The reactive power controller performs two-stage comparisons. In the first stage, PCC reactive power is compared with the load reactive power requirement. In the second stage, the difference is further compared with the controlled deviation of PCCRMS voltage with its corresponding reference. The output is then fed as a reactive power control input. Both EV-ESS charge/discharge controller and reactive power controller are utilized in a simulated hybrid AC/DC micro-grid which is developed mimicking the real micro-grid in Griffith University, Nathan campus to prove controllers' superior performance under variable loading and variable irradiation as shown in fig 1.

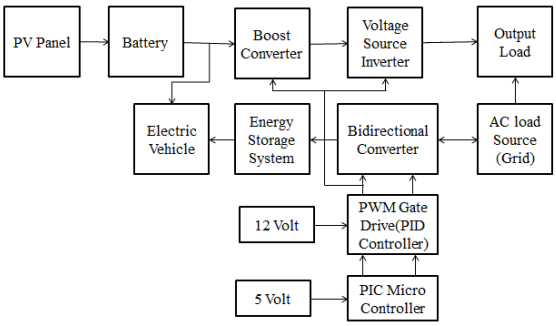

Fig. 1 Block diagram of Proposed System

IV. IMPLEMENTATION

A hybrid AC/DC micro-grid is the combination of AC and DC networks as shown in Figure. Where various AC and DC sources and loads are connected to the corresponding DC and AC networks through transformers and converters, respectively. The DC and AC networks are connected together through the bidirectional AC/DC converters which may be transformerless or with the transformer. The PV conversion systems and fuel cell generators are connected to the DC network through DC/DC boosters. Light wind turbine which needs the battery as energy buffer can also be connected to DC network. DC loads such as electric vehicles (EVs) and LEDs are connected to the DC network through DC/DC buck converters. Power electronics driven AC motors are connected to the DC network through DC/AC converters. DC energy storages such as batteries and supercapacitors are connected to the DC network through bidirectional DC/DC converters. AC power generators such as wind turbine generators and small diesel generators are connected to the AC network. AC energy storages such as flywheels are connected to the AC grid through AC/AC converters. AC loads such as AC motors and heaters are connected to the AC network. The three-phase AC network of the hybrid grid can also be existing in the low-voltage distribution network. The hybrid grid can be an isolated grid or connected to the utility grid through a transformer. It should be noted that a transformer may be required for the connection of some AC sources and loads if their output or input voltages are different from the AC network. The voltage level of the AC grid is 400 V. There is still no standard voltage level for the DC network. The common voltage level currently used in most test systems is 380 V.

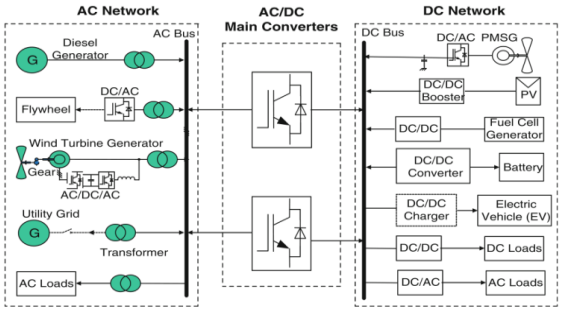

Fig. 2 A typical hybrid AC/DC micro-grid configuration

The designed hybrid AC/DC micro-grid includes two types of controller proposed as interlinking voltage source controller and EV-ESS charge/discharge controller. Overall control strategies are depicted in Fig. 2. In this section, a brief overview of the structures and strategies of these controllers are presented.

A. Interlinking converter controller

The interlinking converter consists of four interconnected subsystems.

1) Phase-locked loop (PLL) measurement

Measured grid side voltage (V_{abc}) is fed to a PLL to get instantaneous angle measurement which is later fed into abc/dq0 converter. Measured grid side voltage (V_{abc}) and current (I_{abc}) are passed through abc/dq0 converter to get corresponding d and q axis components i.e. V_d, V_q, I_d, and I_q.

2) DC Bus voltage regulator

The objective of this subsystem is to regulate DC bus voltage and to generate reference value for the active power control input i.e, $I_{d(ref)}$. In order to do so measured DC voltage is compared with its reference voltage (i.e. 600 V) and then passed through a proportional integral (PI) controller to generate control input $I_{d(ref)}$.

3) Proposed reactive power controller

Active and reactive power of a non-inertial system can be controlled by I_d and I_q respectively. The main task of the proposed reactive power controller is to generate reference value for I_q which is $I_{q(ref)}$. The controller compares PCC reactive power (QPCC) with required load reactive power (Q_{Load}) and the result passed through a PI controller. PCC RMS voltage is also compared with its reference value which in this case in 230Vrms and the result is passed through

International Journal of Engineering Research & Technology (IJERT)
ISSN: 2278-0181
Vol. 8 Issue 04, April-2019

another PI controller. Both results are again compared and passed through another controller to generate $I_{q(ref)}$.

4) Current regulator

The main task of the current regulators to compare Id and I_q with their associated references (ref) and $I_{q(ref)}$ and decouple active and reactive power control from each other. As a result, controller performance becomes independent of system dynamics.

B. Proposed EV-ESS charge/discharge controller

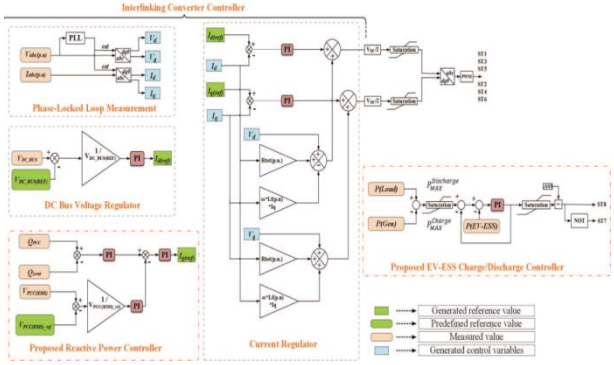

Fig. 3 EV-ESS charge /Discharge controller

V. MODELING AND CONTROL OF PHOTOVOLTAIC SYSTEM

One type of DC power sources is PV panels. Individual PV conversion systems have been well studied and the related techniques have been investigated. A PV panel is simulated as a current source connected in parallel with a diode and a resistor RP and in series with resistor RS shown in Fig. 3.

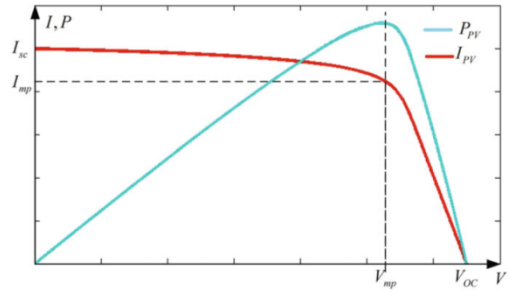

Fig. 4 V-I and P-V curves of a PV panel

$$I_{PV} = n_p I_{ph} - n_p I_{sat}\, X \left[exp\left(\frac{q}{AkT}\left(\frac{V_{PV}}{n_S} + I_{PV} R_S\right)\right) - 1\right]$$

$$I_{ph} = \left(I_{SSO} + k_i(T - T_r)\right) X \frac{S}{1000}$$

$$I_{sat} = I_{rr}\left(\frac{T}{T_r}\right)^3 exp\left(\left(\frac{qE_{gap}}{kA}\right) X \left(\frac{1}{T_r} - \frac{1}{T}\right)\right)$$

where V_{PV} is the terminal voltage of PV panel, I_{ph} is the photocurrent, I_{sat} is the saturation current, q is the electron charge, A is the ideality factor, k is the Boltzmann constant, I_{sso} is the short circuit current, k_i is the short circuit current temperature coefficient, T_r is the reference temperature, I_{rr} is the reverse saturation current at T_r, E_{gap} is the gap energy, np is the number of parallel solar cells, ns is the number of series solar cells, S is the solar irradiation level and T is the junction temperature. The output power of a PV panel depends on the V-I curve as shown in Fig. 4. Where I_{sc} and Voc are the short circuit current and open-circuit voltage, respectively. Because of the nonlinear relationship between the output current and the terminal voltage described in the Equation, the output power PPV changes with the output current. A Maximum Power Point (MPP) exists at the terminal voltage V_{mp} and the output current Imp. Therefore, a PV panel should be controlled to operate at the MPP. A PV panel is connected to the DC bus through a DC/DC bucker, booster or buck–boost converter which depends on the terminal voltage of the panel and the DC bus voltage. The layout and control schematic diagram of a basic DC/DC booster for the integration of a PV system is shown below in Fig 5.

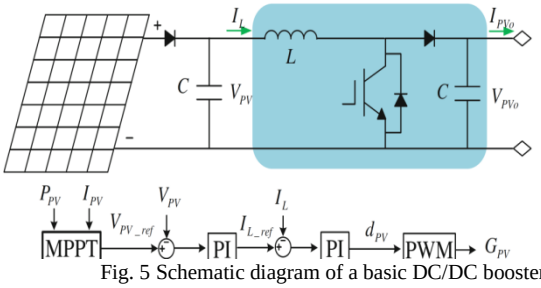

Fig. 5 Schematic diagram of a basic DC/DC booster

The PV system is normally controlled to operate in MPPT mode to harness the maximum power. The MPPT techniques including Perturbation & Observe (P&O), Incremental Conductance (IC), fractional open-circuit voltage, etc., have been well developed and introduced. The reference terminal voltage VP_{V_ref} is generated in the MPPT function block as shown in the figure and tracked by the conventional double-loop PI controller. In the outer voltage loop, the actual terminal voltage V_{PV} is compared with VP_{V_ref} and the error is processed with the PI controller to generate the reference inductor current I_{L_ref}. The inductor current is tracked by a PI controller to generate the duty ratio d_{PV} which is sent to the pulse-width-modulation (PWM) generator to produce the switching signal G_{PV} for generating the maximum power.

VI. MODELING AND CONTROL OF BATTERY ENERGY STORAGE

Battery energy storage system (BESS) is usually designed and connected to the DC bus to maintain the power balance between power generation and loads in the DCC network. The integration techniques of BESSs to AC and DC micro-grids have been well developed. A Bidirectional DC/DC converter is used to interface the battery bank output with the DC bus. The layout and control schematic diagram of a DC/DC buck-boost converter for battery control is as shown in Figure. The converters controlled as a booster when the battery operates in discharging mode and a bucker in charging mode. The upper and lower switches in Figures are controlled to operate in a complementary manner with certain dead-time to prevent short circuit fault. The relationship between the converter output voltage V_{bo} and the battery output voltage V_b is as

$$V_{b0} = \begin{cases} \dfrac{1}{1 - d_{b1}} V_0 (discharging) \\ \dfrac{1}{d_{bu}} V_0\ (Charging) \end{cases}$$

Where d_{bl} and d_{bu} are the duty ratio for the lower and upper switches of the battery converter, respectively.

International Journal of Engineering Research & Technology (IJERT)
ISSN: 2278-0181
Vol. 8 Issue 04, April-2019

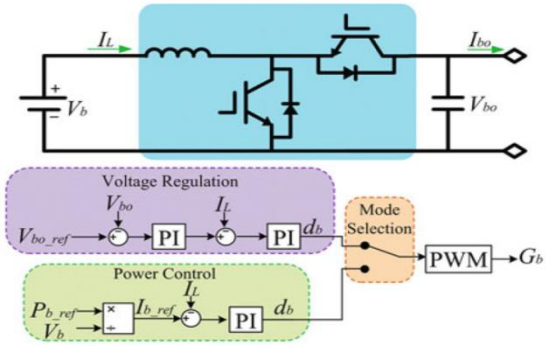

Fig. 6 circuit and the control block diagram of a bidirectional battery converter

Battery converter can be controlled to operate in both voltage regulation and power control modes. In the voltage regulation mode, the reference voltage V_{bo_ref} of the battery converter is defined. The conventional double-loop PI control is implemented to track the reference voltage. BESS maintains system power balance autonomously through charge and discharge. The battery output power P_{b_ref} is defined in the power control mode. Reference battery output current I_{b_ref} is obtained by dividing the power reference with battery terminal voltage. The battery converter duty ratio is generated in the current control loop with the PI controller as shown in above Fig. 6.

VII. LOCAL POWER SHARING IN THE AC NETWORK

WTGs in the AC network is controlled to operate in MPPT mode. The power balance between generation and load is maintained by controlling the outputs from the conventional DGs (CDGs). Power sharing among the CDGs can be realized by the droop control method. The P-f droop curve for x^{th} CDG unit can be expressed as below

$$f = f^* + m_x P_{ac\_x}$$

$$m_{x=\frac{f_{min}-f_{max}}{P_{ac-x}^{max}}}$$

Where f* is the reference frequency of the AC network, P_{ac_x} is power output, mx is the droop coefficient, f_{min} and f_{max} are the minimum and maximum allowable frequency respectively, and P^{max}_{ac} x is the maximum active power. Based on the same system frequency for all DGs, the power-sharing among u CDGs can be obtained as

$$\frac{P_{ac\_1}}{P_{ac\_1}^{max}} = \frac{P_{ac\_2}}{P_{ac\_2}^{max}} = \cdots = \frac{P_{ac-u}}{P_{ac-u}^{max}}$$

VIII. LOCAL POWER SHARING IN THE DC NETWORK

As discussed in the previous section, all the renewable sources are controlled to operate in MPPT mode. The DC bus voltage is maintained by charging or discharging of BESSs. The droop control is applied for power sharing among BESSs. The droop curve of yth BESS in the DC network is as

$$V_{dc\_y} = V_{dc}^* + d_y P_{dc\_y}$$

$$d_y = \frac{V_{dc}^{min} - V_{dc}^{max}}{P_{dc\_y}^{max}}$$

Where V_{dc} is the reference DC bus voltage and configured as the maximum allowable voltage, V_{dc_y} is the terminal voltage of BESS and dy is the negative drop coefficient, V^{min}_{dc} and V^{max}_{dc} are the minimum and maximum allowable DC bus voltage in the DC network, respectively, and P^{max}_{ac} y the is maximum output power for y^{th} BESS. The terminal voltages of BESSs are slightly different with bus voltage V_{dc} due to the different voltage drop in the cable. The voltage difference would lead to inaccurate power-sharing among BESSs. To solve this problem in the DC network, a modified droop equation is developed as,

$$V_{dc\_y} = V_{dc}^* + d_y P_{dc\_y} + i_{dc\_y} Z_{dc\_y}$$

Where i_{dc_y} and Z_{dc_y} are the output current and cable impedance. The power sharing equation among v BESSs can be obtained as

$$\frac{P_{dc\_1}}{P_{dc\_1}^{max}} = \frac{P_{dc\_2}}{P_{dc\_2}^{max}} = \ldots = \frac{P_{dc\_v}}{P_{dc\_v}^{max}}$$

Global Power Sharing Among AC and DC Networks Based on the DC bus voltage and frequency of the AC network, the control algorithm for power exchange between two networks is required. Because of the complexities of control and power-sharing in two networks, a normalization process is proposed to determine the control parameters of the bidirectional converter. The two separate droop characteristics are normalized and combined to determine the power transfer between AC/DC networks. Considering uCDGs in the AC network, the combined AC droop characteristics of the AC network is as

$$f = f^* + M \sum_{x=1}^{u} P_{ac\_x}$$

$$M = 1 \Big/ \sum_{x=1}^{u} \frac{1}{m_x}$$

Where the total active power is generated from u CDG units. M is the combined droop coefficient of the AC network. Considering all BESSs in the DC network, the combined DC droop characteristics of DC network areas. The control scheme based on ensuring that all DGs in AC or DC networks can share a total load of the hybrid grid in proportion to their maximum powers throughout the hybrid AC/DC system.

IX. SIMULATION DIAGRAM

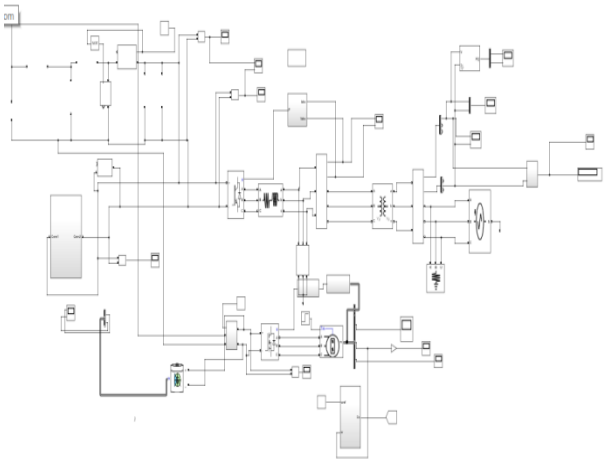

Fig. 7 Simulation Diagram

International Journal of Engineering Research & Technology (IJERT)
ISSN: 2278-0181
Vol. 8 Issue 04, April-2019

Here, we have drawn the simulation diagram with the help of MATLAB software. In this solar panel, resistors, capacitors, inductor and MOSFET etc. were incorporated in the software.

X. RESULTS AND DISCUSSION

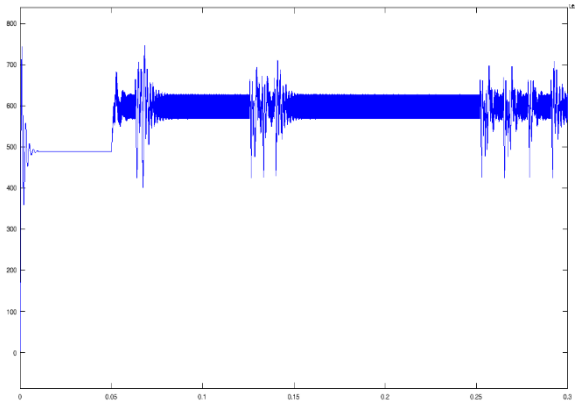

Fig. 8 Output Voltage of Solar Panel Waveform

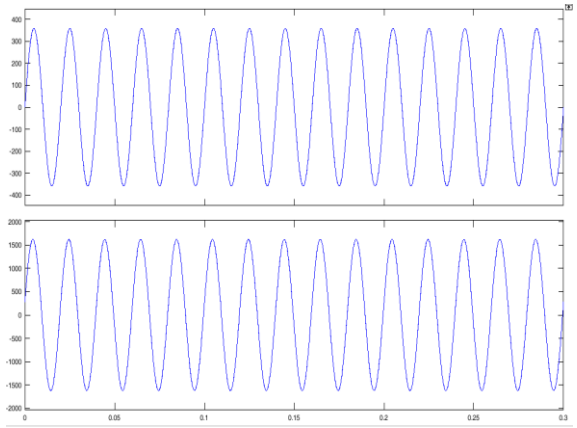

Fig. 9 Grid Voltage and Current Waveform

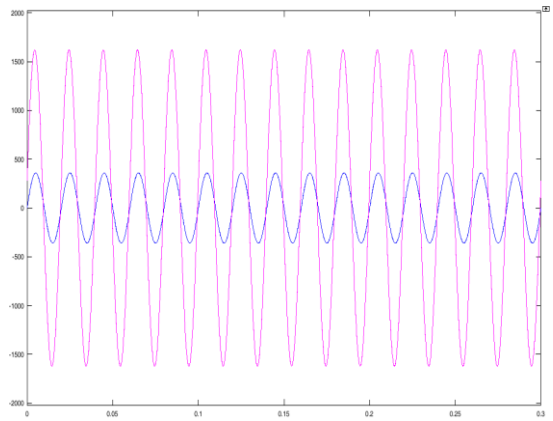

Fig. 10 Grid Voltage and Current power factor waveform

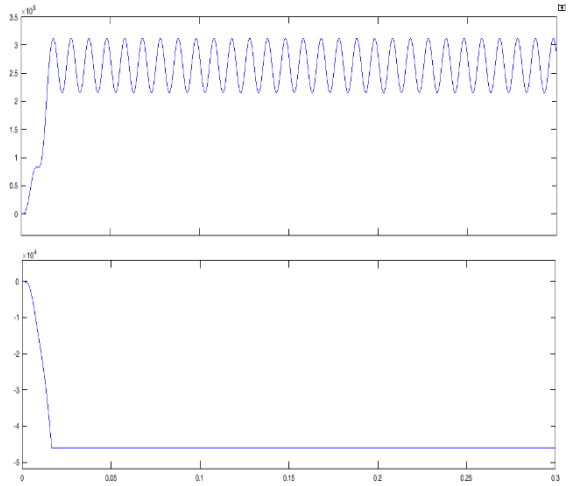

Fig.11 Active Power and Reactive Power waveform

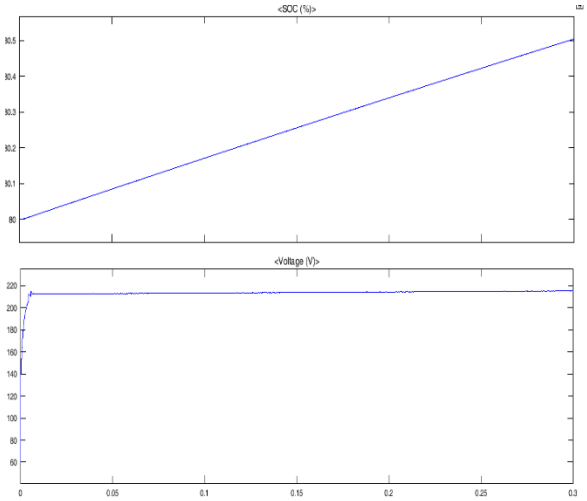

Fig. 12 Battery Voltage and Efficiency waveform

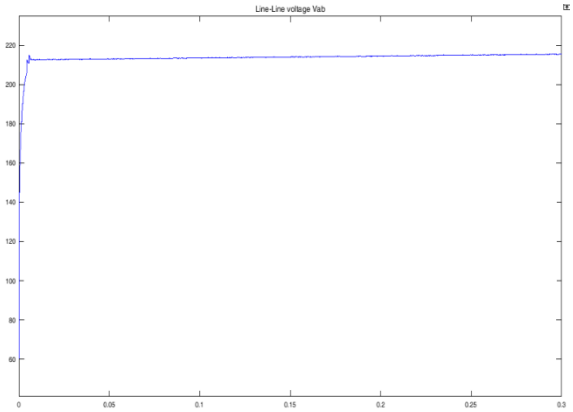

Fig. 13 Bidirectional Converter Voltage waveform

International Journal of Engineering Research & Technology (IJERT)
ISSN: 2278-0181
Vol. 8 Issue 04, April-2019

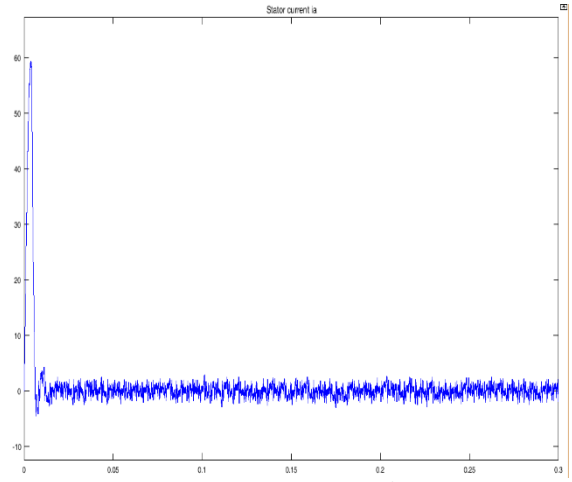

Fig. 14 Stator Current waveform

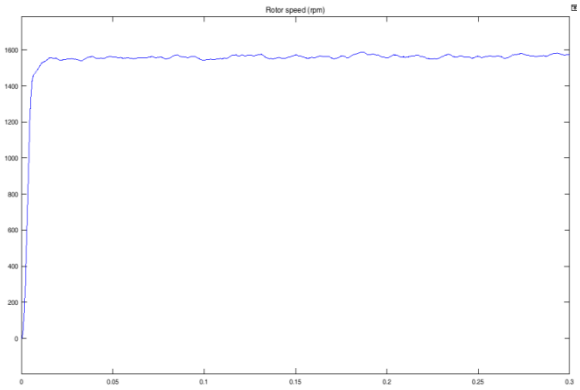

Fig.15 Output Rotor Speed (RPM) waveform

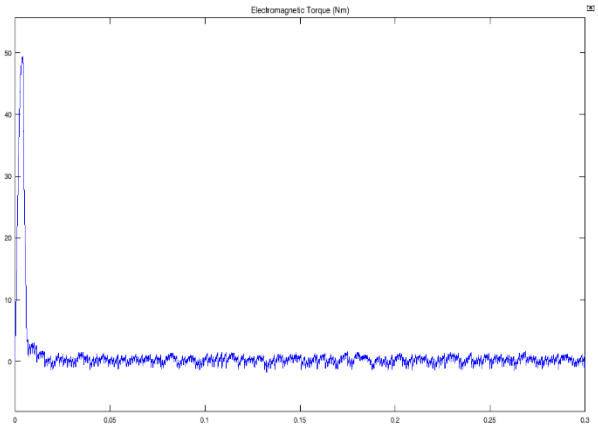

Fig. 16 Output Torque (NM) waveform

XI. CONCLUSION

Thus a novel reactive power controller has been proposed which operates based on the manipulation of PCC reactive power and PCC RMS voltage with their associated references. Here, we are proposed how to manage the power flow between sub-grids and hybrid micro-grids (AC and DC). According to Mitsubishi Outlander, Battery packs has been rearranged for accurate PHEV specification simulation result and also designed to maintain overall control of the system and stabilize voltages of corresponding buses. Simulation results show that both reactive power controller and EV-ESS charge/discharge controller efficiently manage reactive and active power respectively within the designed system. The effects of a wind gust on DFIG WT, the uncertainty of PHEV charging pattern and multiple pair of DC and AC buses have not been considered in this paper, which can be identified as future scopes of this research.

REFERENCES

[1] X. Liu, P. Wang, and P. C. Loh, "A hybrid ac/dc microgrid and itscoordination control," *IEEE Transactions on Smart Grid*, vol. 2, no.2, pp. 278–286, Jun. 2011, ISSN: 1949-3053.

[2] P. C. Loh, D. Li, Y. K. Chai, and F. Blaabjerg, "Autonomous controlof interlinking converter with energy storage in hybrid ac x2013;dcmicrogrid," *IEEE Transactions on Industry Applications*, vol. 49, no.3, pp. 1374–1382, May 2013, ISSN: 0093-9994.

[3] M. Yilmaz and P. Krein, "Review of the impact of vehicle-to-grid technologies on distribution systems and utility interfaces," *IEEE Transactions on Power Electronics*, vol. 28, no. 12, pp. 5673–5689,Dec. 2013, ISSN: 0885-8993.

[4] S.Y. Derakhshandeh, A. S. Masoum, S. Deilami, M. A. S. Masoum,and M. E. HamedaniGolshan, "Coordination of Generation Schedulingwith EVs Charging in Industrial Microgrids," *IEEE Transactionson Power Systems*, vol. 28, no. 3, pp. 3451–3461, Aug. 2013, ISSN:0885-8950.

[5] L. Jian, H. Xue, G. Xu, X. Zhu, D. Zhao, and Z. Y. Shao, "Regulated Charging of Plug-in Hybrid Electric Vehicles for Minimizing Load Variance in Household Smart Micro grid," *IEEE Transactions on Industrial Electronics*, vol. 60, no. 8, pp. 3218–3226, Aug. 2013,ISSN: 0278- 0046.

[6] S. Beer, T. Gomez, D. Dallinger, I. Momber, C. Marnay, M. Stadler,and J. Lai, "An Economic Analysis of Used Electric Vehicle BatteriesIntegrated Into Commercial Building Microgrids," *IEEE Transactionson Smart Grid*, vol. 3, no. 1, pp. 517–525, Mar. 2012, ISSN: 1949-3053.

[7] *Outlander PHEV Specifications - Mitsubishi Motors Australia*. [Online].Available: http : / /www. mitsubishi - motors .com. au / vehicles /outlander-phev/specifications (visited on 03/31/2015).

[8] F. Katiraei and M. Iravani, "Power management strategies for a microgridwith multiple distributed generation units," *IEEE Transactionson Power Systems*, vol. 21, no. 4, pp. 1821–1831, Nov. 2006, ISSN:0885-8950.

[9] N. Eghtedarpour and E. Farjah, "Power control and management ina hybrid ac/dc microgrid," *IEEE Transactions on Smart Grid*, vol. 5,no. 3, pp. 1494–1505, May 2014, ISSN: 1949-3053.